Published in final edited form as:
J Nat Prod. 2012 December 28; 75(12): 2216–2222. doi:10.1021/np300711e.

Glycolysis Inhibitor Screening Identifies the Bis-geranylacylphloroglucinol Protonophore Moronone from *Moronobea coccinea*

Sandipan Datta[†], **Jun Li**[†,‡], **Fakhri Mahdi**[†], **Mika B. Jekabsons**[§], **Dale G. Nagle**[*,†,⊥], and **Yu-Dong Zhou**[*,†]

[†]Department of Pharmacognosy, School of Pharmacy, University of Mississippi, University, Mississippi 38677, United States

[⊥]Research Institute of Pharmaceutical Sciences, University of Mississippi, University, Mississippi 38677, United States

[§]Department of Biology, University of Mississippi, University, Mississippi 38677, United States

Abstract

Tumor cells exhibit enhanced glucose consumption and lactate production even when supplied with adequate oxygen (a phenomenon known as the Warburg effect, or aerobic glycolysis). Pharmacological inhibition of aerobic glycolysis represents a potential tumor-selective approach that targets the metabolic differences between normal and malignant tissues. Human breast tumor MDA-MB-231 cells were used to develop an assay system to discover natural product-based glycolysis inhibitors. The assay employed was based on hypersensitivity to glycolytic inhibition in tumor cells treated with the mitochondrial electron transport inhibitor rotenone. Under such conditions, ATP supply, and hence cell viability, depends exclusively on glycolysis. This assay system was used to evaluate 10,648 plant and marine organism extracts from the U.S. National Cancer Institute's Open Repository. Bioassay-guided isolation of an active *Moronobea coccinea* extract yielded the new *bis*-geranylacylphloroglucinol derivative moronone (**1**). Compound **1** exhibited enhanced antiproliferative/cytotoxic activity in the presence of rotenone-imposed metabolic stress on tumor cells. Surprisingly, mechanistic studies revealed that **1** did not inhibit glycolysis, but rather functions as a protonophore that dissipates the mitochondrial proton gradient. In the presence of rotenone, tumor cells may be hypersensitive to protonophores due to increased ATP utilization by the ATP synthase.

Deregulated cellular energetics, a hallmark of cancer, represents a potential therapeutic target.[1] Tumor cells reprogram their glucose metabolism to rely largely on glycolysis for their energy need, even in the presence of adequate oxygen. This phenomenon is known as the Warburg effect, or `aerobic glycolysis.' Relative to oxidative phosphorylation (OxPhos), aerobic glycolysis is a less efficient means of producing ATP. Tumor cells with high aerobic glycolysis rates are associated with poor prognosis, aggressiveness, and resistance to standard therapeutic regimens.[2–6] It is hypothesized that aerobic glycolysis constitutes an advantageous metabolic environment for unrestricted cell proliferation and tumor growth.[7–9]

[*]**Joint Corresponding Authors** Tel: (662) 915-7026. Fax: (662) 915-6975. dnagle@olemiss.edu (D.G.N.). Tel: (662) 915-7026. Fax: (662) 915-6975. ydzhou@olemiss.edu (Y.-D.Z.)..
[‡]**Present Addresses** Modern Research Center for Traditional Chinese Medicine, Beijing University of Chinese Medicine, Beijing 100029, People's Republic of China.

Supporting Information. The effects of rotenone and 2-DG combinations on MDA-MB-231 cell viability and NMR spectra of **1**. The material is available free of charge via the internet at http://pubs.acs.org.

The concept of targeting tumor metabolism has gained considerable attention over the last two decades[10] and exploratory studies are examining the therapeutic potential of inhibitors that target important enzymes required for aerobic glycolysis.[11] Small-molecules that target aerobic glycolysis, such as 2-deoxy-D-glucose (2-DG) and lonidamine, have entered clinical evaluation in patients with refractory tumors.[12,13] Phase I clinical trials with 2-DG monotherapy showed initial success; however, the phase II clinical trial was terminated due to slow accrual.[12b] Hence, the discovery of potent and mechanistically diverse natural products that target aerobic glycolysis may contribute significantly to the development of tumor-selective agents for cancer treatment.

Natural products are widely recognized as an important source of new anticancer agents.[14] To discover natural product-derived glycolysis inhibitors, a human breast tumor MDA-MB-231 cell-based assay system was established. Lipid extracts (10648 total) from the U.S. National Cancer Institute's (NCI) Open Repository of plant and marine invertebrate extract samples were evaluated in the MDA-MB-231 cell-based assays. Initial chemical isolation studies focused on an active *Moronobea coccinea* Aubl. (Clusiaceae) extract. At first, polycyclic polyprenylated acylphloroglucinol derivatives were believed to be responsible for this glycolysis inhibitory activity.[16] The polyprenylated benzophenones and other acylphloroglucinol derivatives isolated from Clusiaceae plants have been shown to exhibit a wide spectrum of bioactivities (cytotoxic, antimicrobial, antioxidant, and anti-inflammatory).[17] Bioassay-guided isolation led to the discovery of moronone (**1**), an acylphloroglucinol derivative with a previously unreported *bis*-geranyl-substituted carbon skeleton.

RESULTS AND DISCUSSION

Simultaneously inhibiting both glycolysis and OxPhos enhances breast and colon tumor cell cytotoxicity, relative to the effects observed by selectively blocking only one of these metabolic pathways.[18,19] Our working hypothesis was that novel glycolysis inhibitors can be identified by assaying natural products for enhanced antiproliferative activity/cytotoxicity in the presence of an OxPhos inhibitor, relative to the effect produced by the active extract/compound alone. Human breast tumor MDA-MB-231 cells were selected as an in vitro model. The highly glycolytic triple-negative MDA-MB-231 cell line lacks estrogen receptor (ER), progesterone receptor (PR), human epidermal growth factor receptor 2 (HER-2), and exhibits a hormone refractory phenotype that closely resembles advanced stage malignant tumors.[20] The compounds 2-deoxy-D-glucose (2-DG) and rotenone were selected as prototypical glycolysis and OxPhos inhibitors, respectively. Concentration-response studies were performed to determine the effects of 2-DG and rotenone (alone and combined) on MDA-MB-231 cell proliferation/viability following 48 h compound treatment (Figure S1, Supporting Information). At the concentrations tested (0.001 to 0.1 μM, in half-log increments), rotenone had minor effects on MDA-MB-231 cell viability at higher concentrations (7% inhibition at 0.1 μM). However, rotenone did exert maximal inhibition of MDA-MB-231 cellular respiration at 0.1 μM (85% inhibition).[21] At relatively low concentrations (1 and 3 mM) of 2-DG, MDA-MB-231 cell viability was also modestly affected (4% and 8% inhibition, respectively). Rotenone enhanced the cytotoxic/cytostatic effects of 2-DG in a concentration-dependent manner. At higher concentrations (10 and 30 mM), 2-DG suppressed cell proliferation/viability and rotenone did not further enhance this cytotoxicity (Supporting Information).

The inhibition of MDA-MB-231 cell proliferation/viability produced by rotenone (0.1 μM) and 2-DG (3 mM) was dramatically enhanced when the two compounds were combined (40% inhibition versus the calculated 16% additive response, Figure 1A). Similarly heightened responses were observed when 2-DG was combined with either the

mitochondrial ETC complex III inhibitor antimycin A (1 μM) or the F_1F_0-ATPase inhibitor oligomycin (1 μM), respectively (data not shown). These results support the hypothesis that the simultaneous inhibition of mitochondrial ATP synthesis and glycolysis exerts enhanced antiproliferative/cytotoxic effects by inhibiting both important ATP sources. Profound inhibition of glycolysis (e.g., 10 and 30 mM of 2-DG) may yield cytotoxicity that is independent of mitochondrial ETC inhibition, since such inhibition may severely restrict mitochondrial substrate supply and cause loss of mitochondrial function.

To discover natural product-derived glycolysis inhibitors, the MDA-MB-231 cell-based rotenone-dependent differential antiproliferation/cytotoxicity screening assay was employed. Rotenone was used at the concentration (0.1 μM) that suppressed cellular respiration to force the tumor cells to survive under glycolysis-dependent conditions. A total of 10648 samples from the U.S. National Cancer Institute's Open Repository of plant and marine invertebrate extracts were evaluated in this cellular bioenergetics-based differential cytotoxicity assay. MDA-MB-231 cells were exposed to extract samples (20 μg/mL) in the presence (plate #1) or absence (plate #2) of rotenone (0.1 μM) for 48 h and cell viability was determined by the sulforhodamine B method (flow diagram, Figure 1B). In each plate, both media alone and a positive control were tested in triplicate [positive controls: 2-DG (3 mM) plus rotenone (0.1 μM) for plate #1, and 2-DG (3 mM) for plate #2]. The Z′-factor calculated from the following formula was used as a “quality control” for assay reliability: $Z' = 1 - (3 \text{ X } SD_{media} + 3 \text{ X } SD_{positive\ control})/(mean_{media} - mean_{positive\ control})$.[22] In general, assays with a Z′-factor greater than 0.5 are considered reliable. The distribution of Z′-factor values from the evaluation of 121 extract sample plates (88 samples per plate) in the presence of rotenone are shown in Figure 1C as an example for assay reliability. For primary screening, actives were defined as extracts that inhibited cell viability by ≥ 45% in the presence of rotenone and produced a differential cytotoxicity index of ≥ 1.5 upon the addition of rotenone. Twenty-three active extracts were subjected to confirmatory evaluation with the same assay performed in triplicate. Seven extracts were confirmed active.

The active extract of *M. coccinea* stem wood was subjected to bioassay-guided isolation that resulted in identification of a new active compound that was given the trivial name moronone (**1**). The HREISMS of **1** showed a pseudomolecular ion (*m/z*) at 525.2997 $[M + Na]^+$, suggesting a molecular formula of $C_{33}H_{42}O_4$ (index of hydrogen deficiency = 13). The UV spectrum showed absorptions at 237, 281, and 351 nm indicating the presence of a α,β-conjugated benzophenone chromophore (1,3-diketone system).[23] The IR spectrum supported the presence of an α,β-conjugated carbonyl group (1642 cm^{-1}) and OH groups (3510 cm^{-1}) in **1**. The NMR spectra of **1** contained resonances for a benzophenone group [δ_H 7.84 (2H, d, *J* = 7.2 Hz, H-9, 13), 7.46 (3H, overlapped, H-10, 11, 12); δ_C 198.0 (C-7), 142.0 (C-8), 132.1 (C-11), 130.0 (C-9, 13), 129.1 (C-10, 12)] and two geranyl moieties [δ_H 5.51 (2H, t, *J* = 7.2 Hz, H-2′, 2″), 5.17 (2H, t, *J* = 6.4 Hz, H-6′, 6″), 3.02 (4H, overlapped, H_2-1′, 1″), 2.15 (4H, overlapped, H_2-5′, 5″), 2.07 (4H, overlapped, H_2-4′, 4″), 1.79 (6H, s, H_3-10′, 10″), 1.66 (6H, s, H_3-8′, 8″), 1.56 (6H, s, H_3-9′, 9″); δ_C 139.5 (C-3′, 3″), 132.6 (C-7′, 7″), 125.9 (C-6′, 6″), 120.8 (C-2′, 2″), 41.4 (C-4′, 4″), 39.3 (1′, 1″), 28.2 (C-5′, 5″), 27.0 (C-8′, 8″), 19.0 (C-9′, 9″), 17.9 (C-10′, 10″], that were assigned based on the interpretation of HSQC and HMBC data. In addition, one ketone (δ_C 190.2), one quaternary (δ_C 60.2) and four olefinic (δ_C 196.3, 109.9, 184.6, 100.4) carbon resonances were observed in the ^{13}C NMR spectrum of **1**. Based on the index of hydrogen deficiency, **1** was deduced to contain one additional ring. Six additional carbons were attributed to an α,β-conjugated cyclohexenone moiety as proposed in Figure 2 (partial structure C_1–C_6). The ^1H NMR resonances attributed to partial structure C_1–C_{13} were comparable to those of kolanone,[26] except for the presence of an additional proton singlet (δ_H 6.15) in **1**. The singlet proton was located at C-6, as confirmed by the HMBC correlations between δ_H 6.15 (H-6) and δ_C 190.2 (C-1), 184.6 (C-5), 109.5 (C-2), and 60.2 (C-4). Attachment of the two geranyl groups to

C-4 was established on the basis of HMBC correlations between H-1′ and C-3, C-4, C-5, C-1″, and between H-1″ and C-3, C-4, C-5, C-1′. NOESY correlations between H-2′/2″ (δ_H 5.51) and H-4′/2′ or H-4″/2″ (δ_H 2.07) suggested *E*-configurations of the $\Delta^{2',3'}$- and $\Delta^{2'',3''}$-substituted double bonds. Accordingly, the structure of this *bis*-geranyl-substituted benzophenone derivative was determined to be **1**, and it was named moronone.

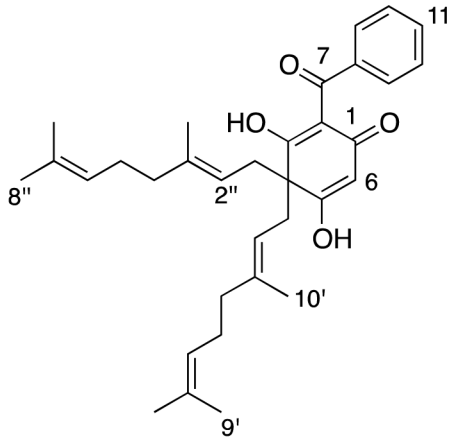

1.

Concentration-response studies were performed to determine the effects of **1** on MDA-MB-231 cell viability in the presence or absence of rotenone (0.1 μM). Rotenone significantly enhanced the cytostatic/cytotoxic activity of **1** at lower concentrations (1, 3, and 10 μM, Figure 3). At 30 μM, **1** suppressed MDA-MB-231 cell proliferation/viability by 68% and rotenone did not further enhance the inhibitory activity (Figure 3). To determine the effects of **1** on cellular bioenergetics, glucose consumption and lactate production by MDA-MB-231 cells were measured in the presence of **1** (1, 3, and 10 μM) after 24 and 48 h treatment. Surprisingly, at 10 μM, **1** significantly increased cellular glucose consumption and lactate production at both time points (Table 1). This suggests that **1** stimulates, rather than inhibits, glycolysis. Rotenone (0.1 μM) enhanced cellular glucose consumption and lactate production, while 2-DG (3 mM) did not significantly impact glucose consumption and lactate production. The relatively low concentration of 2-DG used in this study may contribute to the ineffectiveness of 2-DG at modifying cellular bioenergetics, similar to that observed in the cell proliferation/viability study (Figure S1, Supporting Information). Rotenone and other inhibitors of mitochondrial ETC stimulate glycolysis indirectly by altering the levels of metabolites (e.g., ATP, ADP) that affect glycolytic enzymes. Similarly, compounds that uncouple oxidative phosphorylation have been shown to stimulate glycolytic flux in tumor cells.[24] It is possible that **1** may directly disrupt mitochondrial function.

Compound **1** contains two lipophilic geranyl moieties and proton-exchangeable keto-enolic functionalities. It was hypothesized that **1** may penetrate the mitochondrial inner membrane in both protonated and unprotonated state and act as a protonophore. To test this hypothesis, **1** was first evaluated in MDA-MB-231 and T47D cell-based respiration assays.[25] Compound **1** produced a concentration-dependent biphasic effect on cellular oxygen consumption in both cell lines. At lower concentrations (0.1, 0.3, and 1 μM), **1** increased oxygen consumption, but a decline in respiration rate was observed at a higher concentration (3 μM) (Figure 4A). The prototypical uncoupler FCCP [2-([4-(trifluoromethoxy)phenyl]hydrazinylidene)propanedinitrile, also known as (carbonyl cyanide *p*-trifluoromethoxyphenylhydrazone)] exerted a similar biphasic concentration-dependent effect on cellular respiration (T47D;[26] MDA-MB-231, Figure 4A). To determine if **1** stimulates cellular oxygen consumption by acting as a protonophore or by increasing

cellular ATP consumption, the effects of **1** on oligomycin-imposed state 4 respiration were evaluated in MDA-MB-231 (Figure 4B) and T47D cells (data not shown). The F_0F_1-ATPase inhibitor oligomycin increases mitochondrial membrane potential by blocking proton re-entry into the mitochondrial matrix that, in turn, suppresses electron flow through the respiratory chain. Protonophores such as FCCP reinitiate oligomycin-stalled respiration by translocating protons through the mitochondrial inner membrane into the mitochondrial matrix. The observation that **1** stimulated state 4 respiration in much the same way as observed with FCCP (Figure 4C) supports the possible action of **1** as a protonophore. To exclude enhanced substrate oxidation as the cause of an increase in state 4 respiration, the effect of **1** on in situ mitochondrial membrane potential was examined using the cationic fluorescent dye tetramethylrhodamine methyl ester ($TMRM^+$). Due to its cationic charge, $TMRM^+$ accumulates in the mitochondrial matrix and the fluorescent intensity correlates with the magnitude of the mitochondrial membrane potential. Protonophores, such as FCCP, dissipate the mitochondrial membrane potential that results in the reduction of fluorescent intensity. Compound **1** decreased mitochondrial membrane potential in MDA-MB-231 and T47D cells, just as that observed with FCCP (Figure 4D). These results support the hypothesis that **1** acts as a protonophore.

The effects of the prototypical protonophore FCCP on cell proliferation/viability and cellular bioenergetics were evaluated for comparison with **1**. In MDA-MB-231 cells, rotenone (0.1 μM) significantly enhanced the cytostatic/cytotoxic effects of FCCP (Figure 5A). Similar to the effect observed in the presence of **1**, FCCP increased both glucose consumption and lactate production by MDA-MB-231 cells in a time- and concentration-dependent manner (24 h, Figure 5B; 48 h, Figure 5C). These results indicate that mitochondrial uncouplers can act synergistically with ETC inhibitors to affect tumor cell viability. The concentration for optimum uncoupling in the cell-based respiration assay was lower than the concentration at which FCCP (1 μM) and **1** (10 μM) showed optimum differential cytotoxicity [≥ 45% cytotoxicity in the presence of rotenone (0.1 μM) with a differential index of ≥ 1.5]. This difference may be due to the lack (respiration assay) or presence (viability assay) of FBS in the different assays, as albumin is known to bind FCCP and other hydrophobic compounds and thus decrease compound availability. Further studies revealed that both **1** and FCCP increased glucose consumption and lactate production in a time- and concentration-dependent manner (Table 1; Figures 5B and 5C). These observations are consistent with a previous report that uncouplers stimulate glycolysis in tumor cells.[24]

The *bis*-geranylacylphloroglucinol derivative **1** disrupted mitochondrial respiration by acting as a protonophore. The ability of lipophilic benzophenone and phloroglucinol derivatives to act as protonophores may explain the general antimicrobial, cytotoxic, and other bioactivities exhibited by these compounds. In the MDA-MB-231 cell-based primary assay system, both FCCP and **1** exhibited increased cytotoxicity in the presence of rotenone, a finding that may be the result of ATP depletion. In the presence of an ETC inhibitor, the F_0F_1-ATPase will consume rather than produce ATP, and addition of an uncoupler will exacerbate this consumption by lowering the proton-motive force. It has been reported that the combination of a mitochondrial electron transport chain (ETC) inhibitor and an uncoupler can deplete cellular ATP and suppress cell viability in mammalian cells.[27] Oligomycin, a F_1F_0-ATPase inhibitor, protected cells from the cytotoxic effect exerted by the combination of mitochondrial respiration inhibitor and uncoupler,[27] indicating that the F_0F_1-ATPase can be a significant consumer of ATP under these conditions. An alternative possibility is that the toxicity of complex I inhibitors in combination with an uncoupler results from a synergistic increase in superoxide production. One study has shown that the combination of an uncoupler with a mitochondrial ETC complex I inhibitor synergistically increased superoxide production, that may lead to elevated cytotoxicity.[28] However, there are also reports indicating that uncouplers reduce the high rates of superoxide production by

quinone site-inhibited complex I.[29–31] It is suggested that ATP depletion is the most likely explanation for this toxicity, but additional studies are needed to further define the mechanism of action.

EXPERIMENTAL SECTION

General Experimental Procedures

Optical rotations were obtained on an AP IV/589-546 digital polarimeter. The UV spectrum was recorded in a Varian 50 Bio spectrophotometer and the IR spectrum was obtained on a Bruker Tensor 27 Genesis Series FTIR. Bruker AMX-NMR spectrophotometers operating at 400 MHz for ^{1}H and 100 MHz for ^{13}C were used to record NMR spectra in d_5-pyridine, and solvent resonances were used as internal references [δ8.74 (s) for ^{1}H and 150.35 (t) for ^{13}C]. The HRESIMS were determined on a Bruker Daltonic micro TOF spectrometer fitted with an Agilent 1100 series HPLC and an electrospray ionization source. Merck $Si_{60}F_{254}$ or $Si_{60}RP_{18}F_{254}$ was used to obtain TLCs. The TLC plates were first observed under UV at 254 nm, then sprayed with ethanolic H_2SO_4 (10%) as a visualizing agent, and heated. HPLC was performed on a Waters system equipped with a 600 controller and a 2998 photodiode array detector. Semi-preparative HPLC column (Phenomenex Luna RP-18, 5 μm, 250 × 10 mm) was employed for isolation. Solvents and formic acid for HPLC were from Fisher unless otherwise specified.

Plant Material, Extraction, and Isolation

M. coccinea stem wood was collected from British Guyana (October 21, 1991) and identified by Dr. S. Tiwari (New York Botanical Gardens, Bronx, NY). A voucher specimen (collection No. 0CKF0401) was deposited at the National Museum of Natural History, Smithsonian Institution, Washington, D.C. The plant material was extracted with CH_2Cl_2-MeOH (1:1). The extract was vacuum-dried and stored at −20 °C in the U.S. National Cancer Institute's Open Repository at the Frederick Cancer Research and Development Center (Frederick, Maryland). The active extract (sample number N063783, 3.0 g) was subjected to Sephadex LH-20 column chromatography (CC). Seven fractions were obtained using step gradients of CH_2Cl_2-MeOH (1:1), CH_2Cl_2-MeOH (1:2), and MeOH. The second fraction [373.1 mg, eluted with CH_2Cl_2-MeOH (1:1), one column volume] was active and separated further by Si gel CC using step gradients of hexanes-EtOAc (6:1, 4:1, 2:1, 1:1, 0:1) into eight subfractions. The column was washed with MeOH. The second subfraction [112.2 mg, eluted with hexanes-EtOAc (6:1)] was active and subjected to TLC analysis. The presence of a UV-active yellow char suggested that the active compound might be similar to the polyprenylated acylphloroglucinol derivatives previously isolated from this plant.[16] The active fraction was dissolved in MeOH and centrifuged. The supernatant was subsequently filtered and subjected to semi-preparative HPLC (Phenomenex Luna RP-18, 5 μm, 250 × 10 mm, MeCN with 0.1% formic acid) [87:13] which yielded **1** (83.5 mg). Compound **1** was determined to be > 95% pure by the percentage of the integrated signal at UV 220 nm.

Moronone (1)

dark brown oil; optically inactive; UV (MeOH) λ_{max} (log ε) 237 (4.29), 281 (4.04), 351 (4.39) nm; IR (NaCl block) ν_{max} 3510, 2968, 2918, 1642, 1566, 1504, 1446, 1384, 1316, 1220, 1105, 1066 cm^{-1}; ^{1}H NMR (pyridine-d_5, 400 MHz) δ 8.85 (1H, br s, -OH), 7.84 (2H, d, J = 7.2 Hz, H-9 and H-13), 7.47 (3H, m, H-10, H-11, and H-12), 6.15 (1H, s, H-6), 5.51 (2H, t, J = 7.2 Hz, H-2′ and H-2″), 5.17 (2H, t, J = 6.4 Hz, H-6′ and H-6″), 3.02 (4H, m, H-1′ and H-1″), 2.15 (4H, m, H-5′ and H-5″), 2.07 (4H, m, H-4′ and H-4″), 1.79 (6H, s, H-10′ and H-10″), 1.66 (6H, s, H-8′ and H-8″), 1.56 (6H, s, H-9′ and H-9″); ^{13}C NMR (pyridine-d_5, 100 MHz) δ 198.0 (C, C-7), 196.3 (C, C-3), 190.2 (C, C-1), 184.6 (C, C-5), 142.0 (C, C-8), 139.5 (2C, C-3′ and C-3″), 132.6 (2C, C-7′ and C-7″), 132.1 (CH, C-11),

130.0 (2CH, C-9 and C-13), 129.1 (2CH, C-10 and C-12), 125.9 (2CH, C-6′ and C-6″), 120.8 (2CH, C-2′ and C-2″), 109.5 (C, C-2), 100.4 (CH, C-6), 60.2 (C, C-4), 41.4 ($2CH_2$, C-4′ and C-4″), 39.3 ($2CH_2$, C-1′ and C-1″), 28.2 ($2CH_2$, C-5′ and C-5″), 27.0 ($2CH_3$, C-8′ and C-8″), 19.0 ($2CH_3$, C-9′ and C-9″), 17.9 ($2CH_3$, C-10′ and C-10″); HRESIMS *m*/*z* 525.2997 $[M + Na]^+$ (calcd. for $C_{33}H_{42}O_4Na$, 525.2981).

MDA-MB-231 Cell-Based Cell Proliferation/Viability Assays

Human breast tumor MDA-MB-231 cells (ATCC) were maintained in RPMI 1640 medium that contained L-glutamine (2 mM, Mediatech), and supplemented with fetal bovine serum (FBS, 10% v/v final concentration, Hyclone) and a mixture of penicillin and streptomycin (pen/strep, 50 units mL^{-1} and 50 μg mL^{-1} final concentrations, respectively, Lonza). To screen for glycolysis inhibitors, MDA-MB-231 cells were plated at the density of 3×10^4 cells per well into 96-well plates in a volume of 100 μL RPMI 1640 medium supplemented with FBS (10% v/v) and pen/strep. After 24 h, test compound/extract was diluted in serum-free RPMI 1640 medium with pen/strep and added in a volume of 100 μL per well. Extract samples were evaluated at the final concentration of 20 μg mL^{-1} and rotenone was added at the final concentration of 0.1 μM as specified. The final concentration of solvent (DMSO) is less than 0.5% (v/v). The cells were incubated at 37 °C for 48 h and cell viability was measured using the sulforhodamine B method.[32] Data were processed as % Inhibition of the untreated control.[25] A differential cytotoxicity index was defined as `% $Inhibition_{sample + rotenone}$/% $Inhibition_{sample}$.' Extracts with a differential cytotoxicity index of ≥ 1.5 and ≥ 45% inhibition of cell proliferation/viability in the presence of rotenone were considered active.

Cell-based Respiration Assay

Oxygen consumption in MDA-MB-231 and T47D cells were measured using an Oxytherm Clarke-type electrode system (Hansatech) as described.[25] Respiration rate was normalized to that of the untreated control.[26] For mechanistic studies, oligomycin (1 μM) was added to initiate state 4 respiration, followed by **1** or FCCP as specified.

Mitochondrial Membrane Potential Assay

The fluorescent dye TMRM was employed as an indicator for mitochondrial membrane potential as described.[26] MDA-MB-231 and T47D cells loaded with TMRM were treated with compounds for 30 min and live cell imaging was performed with an Axiovert 200M epifluorescence microscope (Zeiss).

Glucose Consumption and Lactate Production Assays

Plating and compound treatment of MDA-MB-231 cells was the same as that described earlier in the cell proliferation/viability section. At the specified time point (24 or 48 h, as appropriate), conditioned media samples were collected, and the levels of glucose and lactate determined by enzyme-based assays. To determine glucose concentration in the conditioned media, sample (6 μL) was added to reaction buffer (194 μL) that contained triethanolamine (100 mM, pH 7.3), $MgCl_2$ (7 mM), ATP (2 mM), nicotinamide adenine dinucleotide phosphate ($NADP^+$, 2 mM), hexokinase (1 unit mL^{-1}), and glucose-6-phosphate dehydrogenase (1 unit mL^{-1}). The samples were incubated for eight minutes. Following incubation, absorbance at 340 nm was measured on a BioTek Synergy plate reader. Deionized distilled (dd)-water and glucose free RPMI 1640 medium were used as blanks, as appropriate. The amount of glucose in each sample was calculated using the standard curve generated with glucose standards. The level of glucose consumption was determined by subtracting the residual glucose in the conditioned media from that of the cell-free media control, and then normalized to the amount of cellular protein under each

condition. Cellular proteins were extracted with M-PER (Pierce) in the presence of protease inhibitor cocktail (1:10 dilution, Sigma), and the concentration of proteins was determined using a Micro BCA assay kit (Pierce) following manufacturer's instructions.

To determine lactate concentration in the conditioned media, the sample (8 μL) was added to reaction buffer (192 μL) composed of glycylglycine (100 mM, pH 8.0), glutamate (100 mM), nicotinamide adenine dinucleotide (NAD^+, 1 mM), lactate dehydrogenase (LDH, 1 unit mL^{-1}) and glutamate/pyruvate transaminase (1 unit mL^{-1}). The samples were incubated at room temperature for one hour. Following incubation, fluorescence was measured at an excitation wavelength of 340 nm and an emission wavelength of 460 nm on a BioTek Synergy plate reader. Lactate standards were used to generate a standard curve. Data processing and presentation were similar to those described for glucose except that the amount of lactate in the cell-free media control was subtracted from that of the conditioned media sample to obtain the amount of secreted lactate. Enzymes, NAD and NADP were from Calzyme, and other reagents were from Sigma.

Statistical Analysis

Cell viability results were analyzed using two-way ANOVA, followed by Bonferroni post hoc analyses (GraphPad Prism 5). Glucose consumption and lactate production data were analyzed using one-way ANOVA, followed by Dunnett's post hoc analysis. Differences were considered significant when $p < 0.05$.

Supplementary Material

Refer to Web version on PubMed Central for supplementary material.

Acknowledgments

The authors thank the Natural Products Branch Repository Program at the National Cancer Institute for providing extracts from the NCI Open Repository used in these studies, D. J. Newman and E. C. Brown (NCI, Frederick, MD) for assistance with sample logistics and collection information, and Dr. Daneel Ferreira for advice on the structure elucidation. This work was supported in part by the National Institutes of Health National Cancer Institute (grant CA98787) and the National Oceanic and Atmospheric Administration National Institute for Undersea Science and Technology (grant NA16RU1496). This investigation was conducted in a facility constructed with Research Facilities Improvement Grant C06 RR-14503 from the National Institutes of Health.

REFERENCES

(1). Hanahan D, Weinberg RA. Cell. 2011; 144:646–674. [PubMed: 21376230]

(2). Mason EF, Zhao Y, Goraksha-Hicks P, Coloff JL, Gannon H, Jones SN, Rathmell JC. Cancer Res. 2010; 70:8066–8076. [PubMed: 20876800]

(3). Wolf A, Agnihotri S, Micallef J, Mukherjee J, Sabha N, Cairns R, Hawkins C, Guha A. J. Exp. Med. 2011; 208(2):313–326. [PubMed: 21242296]

(4). Zhou M, Zhao Y, Ding Y, Liu H, Liu Z, Fodstad O, Riker AI, Kamarajugadda S, Lu J, Owen LB, Ledoux SP, Tan M. Mol. Cancer. 2011; 9:33. [PubMed: 20144215]

(5). Pitroda SP, Wakim BT, Sood RF, Beveridge MG, Beckett MA, MacDermed DM, Weichselbaum RR, Khodarev NN. BMC Med. 2009; 7:68. [PubMed: 19891767]

(6). Klawitter J, Kominsky DJ, Brown JL, Klawitter J, Christians U, Leibfritz D, Melo JV, Eckhardt SG, Serkova NJ. Br. J. Pharmacol. 2009; 158:588–600. [PubMed: 19663881]

(7). Vander Heiden MG, Cantley LC, Thompson CB. Science. 2009; 324:1029–1033. [PubMed: 19460998]

(8). Kroemer G, Pouyssegur J. Cancer Cell. 2008; 13:472–482. [PubMed: 18538731]

(9). Brand KA, Hermfisse U. FASEB J. 1997; 11:388–395. [PubMed: 9141507]

(10). Papandreou I, Goliasova T, Denko NC. Int. J. Cancer. 2011; 128:1001–1008. [PubMed: 20957634]

(11). Scatena R, Bottoni P, Pontoglio A, Mastrototaro L, Giardina B. Expert Opin. Investig. Drugs. 2008; 17:1533–1545.

(12). a) [(accessed on April 3, 2012)] ClinicalTrials.gov [Internet]. http://clinicaltrials.gov/ct2/show/NCT00096707b) [(accessed on Oct 4, 2012)] ClinicalTrials.gov [Internet]. http://clinicaltrials.gov/ct2/show/NCT00633087

(13). Di Cosimo S, Ferretti G, Papaldo P, Carlini P, Fabi A, Cognetti F. Drugs Today (Barc). 2003; 39:157–174. [PubMed: 12730701]

(14). Newman DJ, Cragg GM. J. Nat. Prod. 2012; 75:311–335. [PubMed: 22316239]

(15). Fantin VR, Leder P. Oncogene. 2006; 25:4787–4797. [PubMed: 16892091]

(16). Marti G, Eparvier V, Moretti C, Susplugas S, Prado S, Grellier P, Retailleau P, Guéritte F, Litaudon M. Phytochemistry. 2009; 70:75–85. [PubMed: 19054532]

(17). Acuña UM, Jancovski N, Kennelley EJ. Curr. Top. Med. Chem. 2009; 9:1560–1580. [PubMed: 19903162]

(18). Cheng G, ZIelonka J, Dranks BP, McAllister D, Mackinnon AC, Joseph J, Kalyanaraman B. Cancer Res. 2012; 72:2634–2644. [PubMed: 22431711]

(19). Fath MA, Diers AR, Aykin-Burns N, Simons AL, Hua L, Spitz DR. Cancer Biol. Ther. 2009; 8:1228–1236. [PubMed: 19411865]

(20). Robey IF, Stephen RM, Brown KS, Baggett BK, Gatenby RA, Gillies RJ. Neoplasia. 2008; 10:745–756. [PubMed: 18670636]

(21). Li J, Mahdi F, Du L, Datta S, Nagle DG, Zhou Y-D. J. Nat. Prod. 2011; 74:1894–1901. [PubMed: 21875114]

(22). Zhang JH, Chung TD, Oldenburg KR. J. Biomol. Screen. 1999; 4:67–73. [PubMed: 10838414]

(23). Hussain RA, Owegby AG, Parimoo P, Waterman PG. Planta Med. 1982; 44:78–81. [PubMed: 7071196]

(24). Sturdík E, Cullý J, Sturdíková M, Durcová E. Neoplasma. 1986; 33:575–582. [PubMed: 3785464]

(25). Liu Y, Veena CK, Morgan JB, Mohammed KA, Jekabsons MB, Nagle DG, Zhou Y-D. J. Biol. Chem. 2009; 284:5859–5868. [PubMed: 19091749]

(26). Du L, Mahdi F, Jekabsons MB, Nagle DG, Zhou Y-D. J. Nat. Prod. 2010; 73:1868–1872. [PubMed: 20929261]

(27). Nieminen AL, Saylor AK, Herman B, Lemasters JJ. Am. J. Physiol. 1994; 267:C67–C74. [PubMed: 8048493]

(28). Cadenas, E.; Han, D. Generation of reactive oxygen species by mitochondria. In: Davies, K., editor. Free Radicals and the Oxygen Paradox: Oxidative Stress in Biology, Aging and Disease. The Biomedical & Life Sciences Collection, Henry Stewart Talks Ltd; London: 2007. online at http://hstalks.com/bio

(29). Brand MD, Buckingham JA, Esteves TC, Green K, Lambert AJ, Miwa S, Murphy MP, Pakay JL, Talbot DA, Echtay KS. Biochem. Soc. Symp. 2004; 71:203–213. [PubMed: 15777023]

(30). Lambert AJ, Brand MD. J. Biol. Chem. 2004; 279:39414–39420. [PubMed: 15262965]

(31). Lambert AJ, Brand MD. Biochem. J. 2004; 382(Pt 2):511–517. [PubMed: 15175007]

(32). Skehan P, Storeng R, Scudiero D, Monks A, McMahon J, Vistica D, Warren JT, Bokesch H, Kenney S, Boyd MR. J. Natl. Cancer Inst. 1990; 82:1107–1112. [PubMed: 2359136]

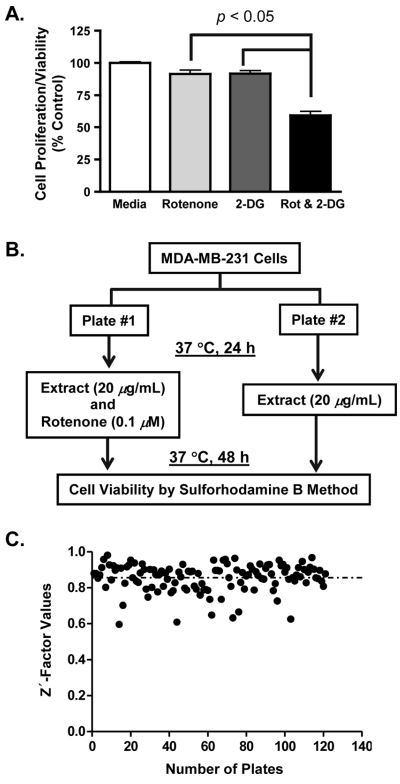

Figure 1.

Development of an MDA-MB-231 cell-based functional assay to identify aerobic glycolysis inhibitors. (A) Effects of rotenone and 2-deoxy-D-glucose (2-DG) on cell proliferation/viability. MDA-MB-231 cells were exposed to 2-DG (3 mM) in the presence or absence of rotenone (0.1 μM) for 48 h. Cell viability was measured by the sulforhodamine B method. Data shown are average + standard deviation from three independent experiments, each performed in duplicate ($n = 6$). The difference between specified groups is considered statistically significant when $p < 0.05$. (B) A schematic flow-diagram of the assay system for the discovery of glycolysis inhibitors. (C) Distribution of Z'-factor values between the media control and 2-DG (3 mM) plus rotenone (0.1 μM) from the evaluation of 121 extract sample plates. The dotted line indicates the average Z'-factor value (0.856) from all the plates.

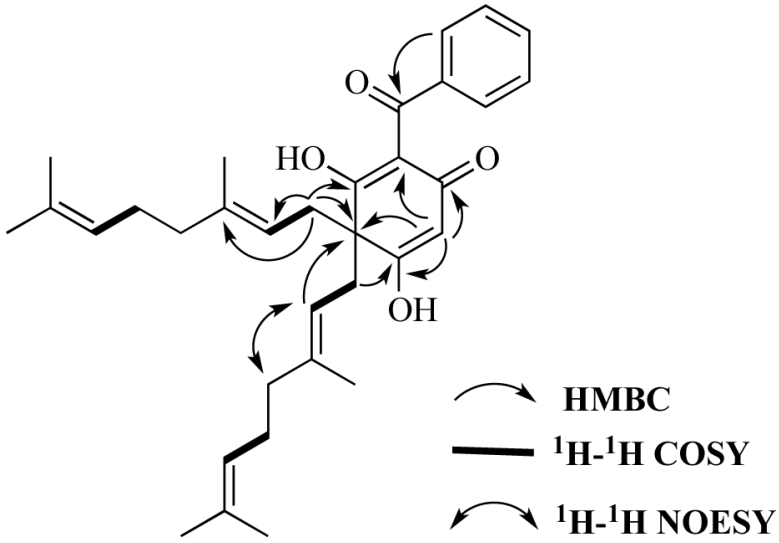

Figure 2.
Selected HMBC, ^{1}H-^{1}H COSY, and NOESY correlations for **1**.

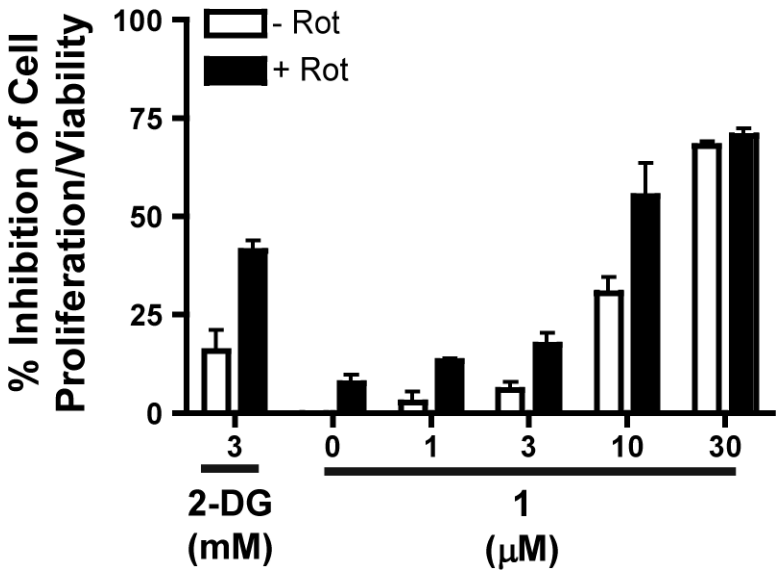

Figure 3.

Differential suppression of MDA-MB-231 cell proliferation/viability by **1** in the absence or presence of rotenone. MDA-MB-231 cells were treated with **1** at the specified concentrations with (solid bar) or without (open bar) 0.1 μM rotenone for 48 h. Data are presented as "% Inhibition" of the untreated control (average + standard deviation from two independent experiments each performed in triplicate, $n = 6$). The glycolysis inhibitor 2-DG (3 mM) was included as a positive control.

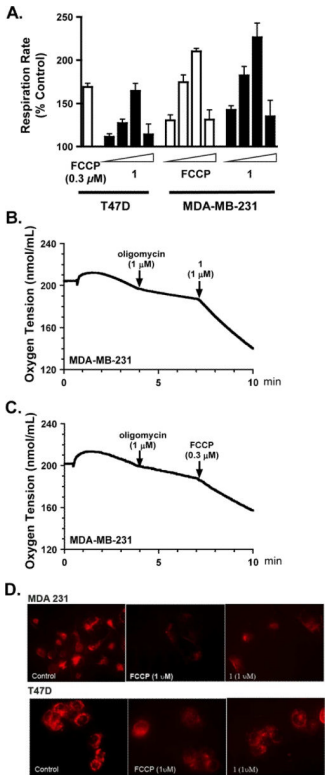

Figure 4.

Effects of **1** on cellular respiration and mitochondrial membrane potential. (A) Concentration-response results of **1** and FCCP on cellular respiration in T47D and MDA-MB- 231 cells. Compound **1** was tested at the concentrations of 0.1, 0.3, 1, and 3 μM. FCCP was evaluated at 0.03 0.1, 0.3, and 1 μM in MDA-MB-231 cells. Oxygen consumption rates in the presence of compounds were normalized to that of the untreated control. Data shown are average + standard deviation from three independent experiments ($n = 3$). (B and C) Compound **1** (1 μM) and FCCP (0.3 μM) stimulated oligomycin-induced state 4 respiration in MDA-MB-231 cells. (D) Dissipation of mitochondrial membrane potential by **1** and FCCP. MDA-MB-231 (upper panel) and T47D (lower panel) cells were loaded with $TMRM^+$ (2 nM, 37 °C for 2 h). The cells were treated with either **1** (1 μM) or FCCP (1 μM) for 30 min, and imaged with an Axiovert 200 M epifluorescence microscope. Images representative of each condition are shown.

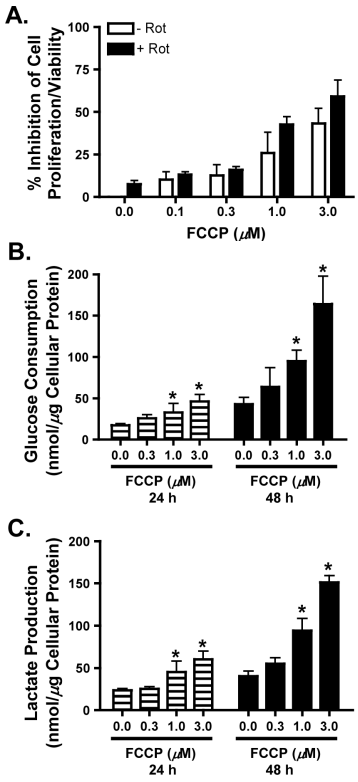

Figure 5.

Concentration-dependent effects of FCCP on MDA-MB-231 cell proliferation/viability, glucose consumption, and lactate production. (A) MDA-MB-231 cells were exposed to FCCP at the specified concentrations with (solid bar) or without (open bar) 0.1 μM rotenone for 48 h and cell viability was determined by the sulforhodamine B method. Data are presented as "% Inhibition" of the untreated control (average + standard deviation from two independent experiments each performed in triplicate). (B) MDA-MB-231 cells were treated with FCCP at specified concentrations for 24 or 48 h. Glucose concentrations in conditioned media were determined by enzyme-based assays and normalized to the amount of cellular proteins. Data shown are average + standard deviation from one representative experiment performed in triplicate. The "*" denotes statistical significance ($p < 0.05$) relative to the untreated control at specified time point. (C) Lactate production by FCCP-treated MDA-MB- 231 cells. Experimental design and data presentation are similar to those described in (B).

Table 1

Effects of **1** on Cellular Glucose Consumption and Lactate Production.[a]

	Glucose Consumed (nmol/μg cellular protein)		Lactate Produced (nmol/μg cellular protein)	
	24 h	**48 h**	**24 h**	**48 h**
untreated control	17.2 ± 2.0	43.0 ± 8.4	23.6 ± 2.0	40.5 ± 6.0
rotenone (0.1 μM)	37.5 ± 7.7*	177.6± 20.1*	75.7 ± 21.8*	190.4 ± 5.6*
2-DG (3 mM)	22.5 ± 2.2	50.2 ± 18.8	26.3 ± 5.1	52.8 ± 6.2
1 (1 μM)	26.7 ± 3.8	44.7 ± 12.9	21.9 ± 4.2	49.3 ± 11.5
1 (3 μM)	25.9 ± 5.3	73.4 ± 5.4*	25.4 ± 3.6	67.3 ± 16.0*
1(10 μM)	45.8 ± 3.0*	168.4 ± 6.5*	59.5 ± 6.4*	168.5 ± 22.2*

[a]MDA-MB-231 cells were treated with test compounds as specified for 24 or 48 h. Glucose and lactate concentrations in conditioned media were determined by enzyme-based assays. Cellular protein concentrations were measured by Micro BCA assay. Data are presented as nmol glucose consumed or nmol lactate produced per μg of cellular proteins (average ± standard deviation) from one representative experiment performed in triplicate. Data were compared using one-way ANOVA and Dunnett's post hoc analyses (GraphPad Prism 5)

*denotes statistical significance ($p < 0.05$) relative to the untreated control.